WCCM V
Fifth World Congress on
Computational Mechanics
July 7–12, 2002, Vienna, Austria
Eds.: H.A. Mang, F.G. Rammerstorfer,
J. Eberhardsteiner

Remarks on Quadrilateral Reissner-Mindlin Plate Elements

Douglas N. Arnold

Institute for Mathematics and its Applications
400 Lind Hall, 207 Church St. SE
University of Minnesota, Minneapolis, MN 55455
e-mail: arnold@ima.umn.edu

Daniele Boffi

Dipartimento di Matematica, Universitè Pavia, 27100 Pavia, Italy
e-mail: boffi@dimat.unipv.it

Richard S. Falk*

Department of Mathematics, Rutgers University, Piscataway, NJ 08854
e-mail: falk@math.rutgers.edu

Key words: Reissner–Mindlin plate, finite element, locking-free, isoparametric

Abstract
Over the last two decades, there has been an extensive effort to devise and analyze finite elements schemes for the approximation of the Reissner–Mindlin plate equations which avoid *locking*, numerical overstiffness resulting in a loss of accuracy when the plate is thin. There are now many triangular and rectangular finite elements, for which a mathematical analysis exists to certify them as free of locking. Generally speaking, the analysis for rectangular elements extends to the case of parallograms, which are defined by affine mappings of rectangles. However, for more general convex quadrilaterals, defined by bilinear mappings of rectangles, the analysis is more complicated. Recent results by the authors on the approximation properties of quadrilateral finite elements shed some light on the problems encountered. In particular, they show that for some finite element methods for the approximation of the Reissner-Mindlin plate, the obvious generalization of rectangular elements to general quadrilateral meshes produce methods which lose accuracy. In this paper, we present an overview of this situation.

1 Introduction

Research over the past twenty years has led to considerable success in obtaining and analyzing finite elements schemes for the approximation of the Reissner–Mindlin plate equations which avoid *locking*, a phenomenon which results in a loss of accuracy when the plate is thin. The finite element schemes for which a mathematical analysis exists to certify them as free of locking are largely restricted to either triangular meshes or rectangular meshes, although the latter are sometimes extended to include the case of parallelogram meshes. While an arbitrary polygon can be "triangulated" by general quadrilaterals, the limitation to rectangles or even parallelograms greatly restricts the type of domains for which such a mesh can be used. Thus, it is important to understand whether the schemes designed for rectangular meshes also work well for more general quadrilateral meshes. As we shall see in this paper, there can be a loss of accuracy when successful finite element methods for approximating the Reissner–Mindlin plate equations are extended in the obvious way to quadrilateral meshes.

We recall that the Reissner–Mindlin plate model determines functions $\boldsymbol{\theta}$ and ω, which are defined on the middle surface Ω of the plate and approximate the rotation vector and transverse displacement, respectively, as the minimizers of the energy functional

$$J(\boldsymbol{\theta},\omega) = \frac{1}{2}\int_\Omega \mathsf{C}\,\mathcal{E}\,\boldsymbol{\theta} : \mathcal{E}\,\boldsymbol{\theta} + \frac{\lambda t^{-2}}{2}\int_\Omega |\boldsymbol{\theta} - \mathbf{grad}\,\omega|^2 - \int_\Omega g\omega$$

over $\mathring{\boldsymbol{H}}^1(\Omega)\times\mathring{H}^1(\Omega)$ (for simplicity we have assumed clamped boundary conditions). Here $\mathcal{E}\,\boldsymbol{\theta}$ denotes the symmetric part of the gradient of $\boldsymbol{\theta}$, g the scaled transverse loading function, t the plate thickness, and $\lambda = Ek/2(1+\nu)$ with E Young's modulus, ν the Poisson ratio, and k the shear correction factor. For all 2×2 symmetric matrices $\mathcal{J}$, $\mathsf{C}\mathcal{J} = \{E/[12(1-\nu^2)]\}[(1-\nu)\mathcal{J} + \nu\,\mathrm{tr}(\mathcal{J})\mathcal{I}]$, where $\mathcal{I}$ is the 2×2 identity matrix.

Many of the finite element schemes which have been proposed to overcome locking take the following form. The approximate solution $(\boldsymbol{\theta}_h,\omega_h)$ is determined in a finite element space $\boldsymbol{\Theta}_h\times W_h$ as the minimizer of a modified energy functional

$$J_h(\boldsymbol{\theta},\omega) = \frac{1}{2}\int_\Omega \mathsf{C}\,\mathcal{E}\,\boldsymbol{\theta} : \mathcal{E}\,\boldsymbol{\theta} + \frac{\lambda t^{-2}}{2}\int_\Omega |\boldsymbol{R}_h\boldsymbol{\theta} - \mathbf{grad}\,\omega|^2 - \int_\Omega g\omega. \tag{1.1}$$

The modification consists of the incorporation of a *reduction operator* $\boldsymbol{R}_h : \boldsymbol{\Theta}_h \to \boldsymbol{\Gamma}_h$, where $\boldsymbol{\Gamma}_h$ is an auxiliary finite element space and $\boldsymbol{R}_h$ is typically either an interpolation operator or an L^2-projection operator. The finite element spaces $\boldsymbol{\Theta}_h$ and W_h may be either conforming or nonconforming. In the latter case, the differential operators in (1.1) must be applied element-by-element. All the schemes discussed in this paper will be of this form. Thus, to specify a particular scheme we need to specify the spaces $\boldsymbol{\Theta}_h$, W_h, and $\boldsymbol{\Gamma}_h$, and the reduction operator $\boldsymbol{R}_h$.

Although the results we obtain can be applied more generally to standard families of elements developed for the approximation of the Reissner-Mindlin plate equations, for ease of exposition we concentrate here on the low order elements of a number of these families. These are described in the next section, first considering the case of triangular finite elements and then discussing rectangular and quadrilateral elements.

As we shall see, a main difficulty in extending rectangular (or even parallelogram elements) to quadrilateral elements is the possible loss of approximation accuracy due to the replacement of the affine map from the reference element (unit square) to a general rectangle (or parallelogram) by the bilinear map

which takes the reference square to a more general quadrilateral. This problem is most easily described in the case of scalar finite elements. Quadrilateral finite elements are usually constructed by starting with a finite dimensional space $\hat{V}$ of shape functions (usually polynomials) given on a reference element $\hat{K}$. If K denotes a typical element in the quadrilateral mesh and $\boldsymbol{F}$ denotes the bilinear mapping taking $\hat{K}$ to K, then we constuct a space of functions $V_F(K)$ on the image element K as the composition of functions in $\hat{V}$ with $\boldsymbol{F}^{-1}$, i.e., for $\hat{v} \in \hat{V}$, define $v \in V_F(K)$ by $v(\boldsymbol{x}) = v(\boldsymbol{F}(\hat{\boldsymbol{x}})) = \hat{v}(\hat{\boldsymbol{x}})$. Now suppose τ_h denotes a family of meshes of quadrilaterals of a domain Ω indexed by the maximum mesh size h, and consider the space V^{τ_h} of functions whose restriction to the element K belong to $V_F(K)$. It is well known that in the case when the mapping $\boldsymbol{F}$ is affine (giving only parallelograms), a necessary and sufficient condition for approximation of order $r+1$ in $L^2(\Omega)$ of smooth functions by functions in V^{τ_h} is that the space $\hat{V}$ of functions on the reference element $\hat{K}$ contain all polynomial functions of total degree r. However, it was shown in [1] that in the case of more general bilinear maps, a necessary condition for approximation of order $r+1$ in $L^2(\Omega)$ is that the space $\hat{V}$ of functions on the reference element $\hat{K}$ contain all polynomial functions of separate degree r. This condition was already known to be sufficient.

One can also examine what is needed for approximation of order $r+1$ in $L^2(\Omega)$ in the case of vector-valued functions defined on a arbitrary quadrilateral by mapping from a reference element using a rotated version of the Piola transform. As we shall explain, such elements enter in a natural way in many of the successful approximation schemes for the Reissner-Mindlin plate. After stating results on necessary conditions for optimal order convergence of these type of approximations, we shall examine their implications for the convergence of the extension to quadrilateral meshes of several well-known elements which have been analyzed for rectangular meshes.

The outline of the paper is as follows. In the next section, we recall some low order finite element schemes for the approximation of the Reissner-Mindlin plate problem using triangular and rectangular elements and discuss their extension to the case of quadrilateral meshes. In Section 3, we state a result which can be used to derive error estimates for such schemes by relating the error in the method to questions in approximation theory. In the following section, we summarize some new results on approximation by quadrilateral finite elements which have implications for the rate of convergence that can be achieved by the quadrilateral finite element schemes. These implications are then discussed in detail in Section 5.

2 Finite element schemes for the Reissner–Mindlin plate

In this section, we recall a variety of finite element schemes for the Reissner–Mindlin plate which have been proposed and analyzed for triangular and rectangular meshes. We then describe their extension to quadrilateral meshes. To describe each scheme, we need only define the finite element spaces $\boldsymbol{\Theta}_h$, W_h, and $\boldsymbol{\Gamma}_h$ and the reduction operator $\boldsymbol{R}_h$.

To simplify the description of the elements, we first introduce some basic notation. Let Ω be a polygonal domain and let $\{\tau_h\}_{0<h<1}$ be a subdivision of Ω into either triangles, rectangles, or quadrilaterals, where the subscript h refers to the diameter of the largest element in the subdivision. For any set K, define $P_k(K)$ as the set of restrictions to K of polynomials of degree at most k, $P_{k_1,k_2}(K)$ as the set of restrictions to K of polynomials of degree at most k_1 in x_1 and at most k_2 in x_2, and $Q_k(K) = P_{k,k}(K)$ as the set of restrictions of polynomials of degree at most k in each variable,

We begin with the case of triangular elements. Although we consider only low order elements, many of these elements have well-known extensions to families of elements of arbitrary order.

Durán–Liberman element:

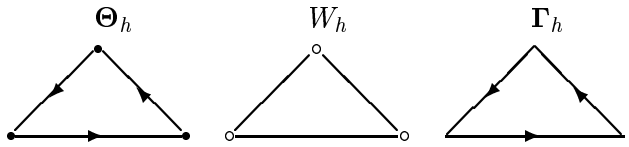

Here $\boldsymbol{\Theta}_h$ is the set of continuous, piecewise linear vectors plus the span of $\lambda_2\lambda_3\,\boldsymbol{\tau}_1$, $\lambda_3\lambda_1\,\boldsymbol{\tau}_2$, $\lambda_1\lambda_2\,\boldsymbol{\tau}_3$, where λ_i are the barycentric coordinates of the triangle and $\boldsymbol{\tau}_i$ are the unit tangent vectors on the triangle sides. W_h is chosen as the space of continuous, piecewise linear functions and $\boldsymbol{\Gamma}_h$ as the rotation of the lowest order Raviart-Thomas space, i.e., on each triangle, functions in $\boldsymbol{\Gamma}_h$ have the form $(a-by, c+bx)$. The reduction operator $\boldsymbol{R}_h$ is defined by the three edge conditions $\int_e \boldsymbol{R}_h\boldsymbol{\gamma}\cdot\boldsymbol{\tau} = \int_e \boldsymbol{\gamma}\cdot\boldsymbol{\tau}$.

Arnold–Falk element:

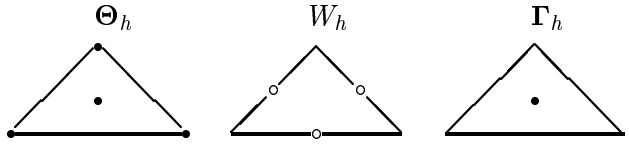

Here $\boldsymbol{\Theta}_h$ is the space of continuous, piecewise linear vectors plus the cubic bubble functions (defined on each triangle by $\lambda_1\lambda_2\lambda_3$). W_h is the space of nonconforming, piecewise linear functions, i.e., piecewise linear functions which are continuous at midpoints of edges. $\boldsymbol{\Gamma}_h$ is the space of piecewise constant vectors, and $\boldsymbol{R}_h$ is defined on each triangle T by the condition $\int_T \boldsymbol{R}_h\boldsymbol{\phi} = \int_T \boldsymbol{\phi}$.

Falk–Tu element:

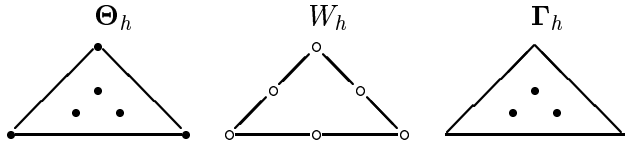

Here $\boldsymbol{\Theta}_h$ is the space of continuous, piecewise linear functions plus quartic bubble functions, (i.e., $\lambda_1\lambda_2\lambda_3(a\lambda_1 + b\lambda_2 + c\lambda_3)$, W_h the space of continuous, piecewise quadratic functions, and $\boldsymbol{\Gamma}_h$ the space of discontinuous piecewise linear vectors. The operator $\boldsymbol{R}_h$ is L^2 projection into $\boldsymbol{\Gamma}_h$.

MITC7 element:

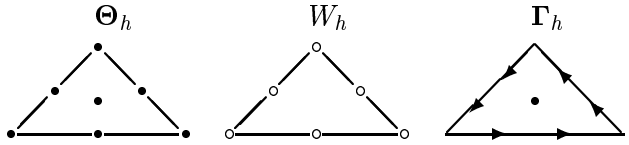

Here $\boldsymbol{\Theta}_h$ is the space of continuous, piecewise quadratic vectors plus cubic bubble functions, W_h is the space of continuous, piecewise quadratic functions, and $\boldsymbol{\Gamma}_h$ is the rotation of the second lowest order Raviart-Thomas space, i.e., on each triangle elements of $\boldsymbol{\Gamma}_h$ have the form $(a+bx+cy-dxy-ey^2, f+gx+hy+exy+dx^2)$. The operator $\boldsymbol{R}_h$ is the standard interpolation operator into $\boldsymbol{\Gamma}_h$ defined by the conditions: $\int_e \boldsymbol{R}_h\boldsymbol{\gamma}\cdot\boldsymbol{\tau}\,p_1 = \int_e \boldsymbol{\gamma}\cdot\boldsymbol{\tau}\,p_1, \forall p_1\in P_1(e)$, $\int_T \boldsymbol{R}_h\boldsymbol{\gamma} = \int_T \boldsymbol{\gamma}$.

A slightly simpler variation of this element can be constructed using the rotated version of the Brezzi-Douglas-Marini elements to approximate $\boldsymbol{\Gamma}_h$. Such an element is mentioned in [4]. We label this the MITC6 element.

MITC6 element:

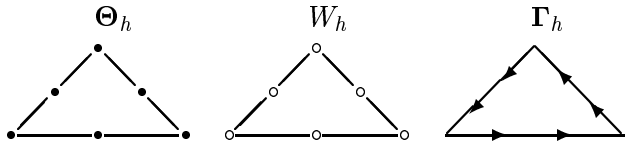

Here $\boldsymbol{\Theta}_h$ is the space of continuous, piecewise quadratic vectors, W_h is the space of continuous, piecewise quadratic functions, and $\boldsymbol{\Gamma}_h$ is the rotation of the space $\boldsymbol{BDM}_1$, consisting on each triangle of vectors with components in P_1. The operator $\boldsymbol{R}_h$ is the standard interpolation operator into $\boldsymbol{\Gamma}_h$ defined by the edge conditions: $\int_e \boldsymbol{R}_h \boldsymbol{\gamma} \cdot \boldsymbol{\tau}\, p_1 = \int_e \boldsymbol{\gamma} \cdot \boldsymbol{\tau}\, p_1, \forall p_1 \in P_1(e)$.

We next consider rectangular elements.

MITC4 element:

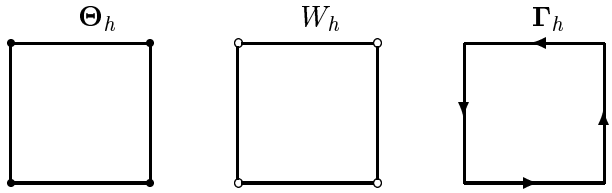

Here $\boldsymbol{\Theta}_h$ is the space of continuous, piecewise bilinear vectors, W_h is the space of continuous piecewise bilinear functions, and $\boldsymbol{\Gamma}_h$ is the rotation of the lowest order Raviart-Thomas space, i.e., on each rectangle, elements of $\boldsymbol{\Gamma}_h$ have the form $(a + by, c + dx)$. The operator $\boldsymbol{R}_h$ is the standard interpolation operator into $\boldsymbol{\Gamma}_h$ defined by the edge conditions $\int_e \boldsymbol{R}_h \boldsymbol{\gamma} \cdot \boldsymbol{\tau} = \int_e \boldsymbol{\gamma} \cdot \boldsymbol{\tau}$.

Durán–Liberman element:

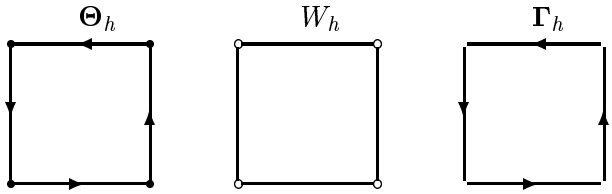

Here $\boldsymbol{\Theta}_h$ is the set of continuous, piecewise bilinear vectors plus the span of the edge bubbles, defined on the unit square by $\hat{x}(1-\hat{x})(1-\hat{y})\,\boldsymbol{\tau}_1$, $\hat{x}\hat{y}(1-\hat{y})\,\boldsymbol{\tau}_2$, $\hat{x}(1-\hat{x})\hat{y}\,\boldsymbol{\tau}_3$, and $(1-\hat{x})\hat{y}(1-\hat{y})\,\boldsymbol{\tau}_4$, where $\boldsymbol{\tau}_i$ are the unit tangent vectors $(1,0)$, $(0,1)$, $(-1,0)$, and $(0,-1)$ on the sides of the unit square. W_h is chosen as the space of continuous, piecewise bilinear functions and $\boldsymbol{\Gamma}_h$ is the rotation of the lowest order Raviart-Thomas space. Note that the only difference between this method and MITC4 is the choice of the space for the rotation vector.

Ye element:

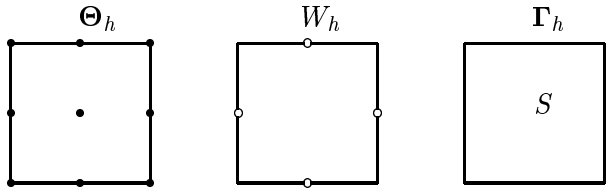

Here $\boldsymbol{\Theta}_h$ is the set of continuous, piecewise biquadratic vectors. W_h is the space of nonconforming (i.e., continuous average values across rectangle edges) rotated bilinear elements defined on the unit square as the span of $\{1, \hat{x}, \hat{y}, \hat{x}^2 - \hat{y}^2\}$. Note that the usual bilinear elements are not uniquely defined by their

average values on the sides of the unit square, since the bilinear function $(\hat{x} - 1/2)(\hat{y} - 1/2)$ has zero average value on the four sides. The space $\boldsymbol{\Gamma}_h$ is chosen to be discontinuous vectors, which on each rectangle have the form $(b + dx, c - dy)$.

MITC8 element:

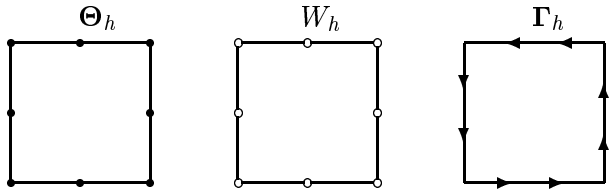

Here $\boldsymbol{\Theta}_h$ is the space of continuous, piecewise serendipity quadratic vectors, W_h is the space of serendipity quadratics, (i.e., continuous functions which on each rectangle are the span of $(1, x, y, xy, x^2, y^2, x^2y, xy^2)$, and $\boldsymbol{\Gamma}_h$ is the rotation of $\boldsymbol{BDM}_1$, the space of Brezzi-Douglas–Marini elements. On each rectangle, elements of $\boldsymbol{\Gamma}_h$ have the form $(a_1 + b_1x + c_1y + 2dxy + ey^2, a_2 + b_2x + c_2y + dx^2 + 2exy)$. The operator $\boldsymbol{R}_h$ is the standard interpolation operator into $\boldsymbol{\Gamma}_h$ defined by the edge conditions $\int_e \boldsymbol{R}_h\,\boldsymbol{\gamma}\cdot\,\boldsymbol{\tau}\,p_1 = \int_e \boldsymbol{\gamma}\cdot\,\boldsymbol{\tau}\,p_1, \forall p_1 \in P_1(e)$.

MITC9 element:

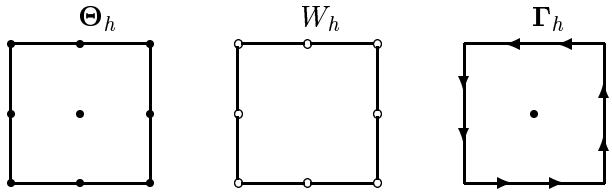

Here $\boldsymbol{\Theta}_h$ is the space of continuous, piecewise biquadratic vectors, W_h is the space of serendipity quadratics, and $\boldsymbol{\Gamma}_h$ is the rotation of $\boldsymbol{BDFM}_2$, the space of Brezzi-Douglas-Fortin-Marini elements. On each rectangle, elements of $\boldsymbol{\Gamma}_h$ have the form $(a_1+b_1x+c_1y+d_1xy+e_1y^2, a_2+b_2x+c_2y+d_2xy+e_2x^2)$. The operator $\boldsymbol{R}_h$ is the standard interpolation operator into $\boldsymbol{\Gamma}_h$ defined by the conditions $\int_e \boldsymbol{R}_h\,\boldsymbol{\gamma}\cdot\,\boldsymbol{\tau}\,p_1 = \int_e \boldsymbol{\gamma}\cdot\,\boldsymbol{\tau}\,p_1, \forall p_1 \in P_1(e)$, $\int_K \boldsymbol{\gamma} = \int_K \boldsymbol{R}_h\,\boldsymbol{\gamma}$.

There is also an analogue of MITC9 based on the rotated version of the Raviart-Thomas ($\boldsymbol{RT}$) elements, which we label MITC12.

MITC12 element:

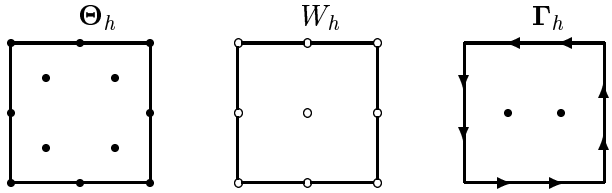

Here $\boldsymbol{\Theta}_h$ is the space of continuous, piecewise biquadratic vectors plus the bicubic bubble functions, which on each rectangle have the form $(1-x)x(1-y)y(ax+by+cxy)$. W_h is the space of continuous biquadratics, and $\boldsymbol{\Gamma}_h$ is the rotation of $\boldsymbol{RT}_1$, the second lowest space of Raviart-Thomas elements. On each rectangle, elements of $\boldsymbol{\Gamma}_h$ have the form $P_{1,2} \times P_{2,1}$. The operator $\boldsymbol{R}_h$ is the standard interpolation operator into $\boldsymbol{\Gamma}_h$ defined by the conditions $\int_e \boldsymbol{R}_h\,\boldsymbol{\gamma}\cdot\,\boldsymbol{\tau}\,p_1 = \int_e \boldsymbol{\gamma}\cdot\,\boldsymbol{\tau}\,p_1, \forall p_1 \in P_1(e)$, $\int_K \boldsymbol{\gamma}\cdot\boldsymbol{q} = \int_K \boldsymbol{R}_h\,\boldsymbol{\gamma}\cdot\boldsymbol{q} \quad \forall \boldsymbol{q} \in P_{1,0} \times P_{0,1}$.

We now consider the extension of these elements to the case of quadrilaterals. We let $\boldsymbol{F}$ be an invertible bilinear mapping from the reference element $\hat{K} = [0,1] \times [0,1]$ to a convex quadrilateral K. For scalar

functions, if $\hat{v}(\hat{\boldsymbol{x}})$ is function defined on $\hat{K}$, we define $v(\boldsymbol{x})$ on K by $v = \hat{v} \circ \boldsymbol{F}^{-1}$. Then, for $\hat{V}$ a set of shape functions given on $\hat{K}$, we define

$$V_F(K) = \{v : v = \hat{v} \circ \boldsymbol{F}^{-1}, \hat{v} \in \hat{V}\}.$$

For all the examples given previously, the space W_h may be defined in this way, beginning with the shape functions denoted in the figures. This preserves the appropriate interelement continuity when the usual degrees of freedom are chosen. The same mapping, applied to each component, can be used with minor exceptions to define the space $\boldsymbol{\Theta}_h$. One exception occurs for the Durán-Liberman element, where one adds to the mapped bilinear vectors a set of four edge bubbles $\{\boldsymbol{p}_1, \boldsymbol{p}_2, \boldsymbol{p}_3, \boldsymbol{p}_4\}$ defined by $\boldsymbol{p}_1(\boldsymbol{F}(\hat{\boldsymbol{x}})) = (\hat{x})(1-\hat{x})(1-\hat{y})\,\boldsymbol{\tau}_1$, where now $\boldsymbol{\tau}_1$ denotes the unit tangent on the edge of K corresponding to the side $\hat{y} = 0$ on the reference square, with analogous definitions for the other $\boldsymbol{p}_i$. There is also the possibility of using a different mapping to define the interior degrees of freedom for the space $\boldsymbol{\Theta}_h$, since this will not affect the interelement continuity.

To define the space $\boldsymbol{\Gamma}_h$, we use a rotated version of the Piola transform. Letting $D\boldsymbol{F}$ denote the Jacobian matrix of the transformation $\boldsymbol{F}$, if $\hat{\boldsymbol{\eta}}$ is a vector function defined on $\hat{K}$, we define $\boldsymbol{\eta}$ on K by

$$\boldsymbol{\eta}(\boldsymbol{x}) = \boldsymbol{\eta}(\boldsymbol{F}(\hat{\boldsymbol{x}})) = [D\boldsymbol{F}(\hat{\boldsymbol{x}})]^{-t}\,\hat{\boldsymbol{\eta}}(\hat{\boldsymbol{x}}),$$

where A^{-t} denotes the transpose of the inverse of the matrix A. Then if $\hat{\boldsymbol{V}}$ is a set of vector shape functions given on $\hat{K}$, we define

$$\boldsymbol{V}_F(K) = \{\,\boldsymbol{\eta} :\, \boldsymbol{\eta} = [D\boldsymbol{F}]^{-t}\,\hat{\boldsymbol{\eta}} \circ \boldsymbol{F}^{-1},\, \hat{\boldsymbol{\eta}} \in \hat{\boldsymbol{V}}\}.$$

For $\omega \in W_h$, $\mathbf{grad}\,\omega = D\boldsymbol{F}^{-t}\hat{\mathbf{grad}}\,\hat{\omega}$. Hence, if on the reference square $\hat{\mathbf{grad}}\,\hat{\omega} \subseteq \hat{\boldsymbol{V}}$, we will also have $\mathbf{grad}\,\omega \subseteq \boldsymbol{\Gamma}_h$, a condition that is needed to guarantee uniqueness of solutions.

Although the extensions to quadrilaterals are in most cases straightforward to define, the question is whether the method retains the same order of approximation as in the rectangular case. To understand this situation, we look in the next section at a method of error analysis originally proposed by Durán and Liberman [11].

3 Error Analysis

In this section, we consider one method of analysis for deriving order of convergence estimates for approximation schemes for the Reissner-Mindlin plate. As is standard in finite element analysis, the aim is first to relate the error in the method to how well the true solution can be approximated by functions in the finite element subspace. The following result is a generalization of a theorem in [11] and can be found in [12].

Theorem: Suppose $\mathbf{grad}\,W_h \subset \boldsymbol{\Gamma}_h$ and let $\omega_I \in W_h$ and $\boldsymbol{\phi}_I \in \boldsymbol{\Theta}_h$. Define

$$\boldsymbol{\gamma} = t^{-2}(\mathbf{grad}\,\omega - \boldsymbol{\phi}), \qquad \boldsymbol{\gamma}_h = t^{-2}(\mathbf{grad}\,\omega_h - \boldsymbol{R}_h\,\boldsymbol{\phi}_h), \qquad \boldsymbol{\gamma}_I = t^{-2}(\mathbf{grad}\,\omega_I - \boldsymbol{R}_h\,\boldsymbol{\phi}_I).$$

Suppose for $s \geq 1$, $\|\boldsymbol{\gamma} - \boldsymbol{R}_h\,\boldsymbol{\gamma}\|_0 \leq Ch\|\boldsymbol{\gamma}\|_1$. Then

$$\|\boldsymbol{\phi} - \boldsymbol{\phi}_h\|_1 + t\|\boldsymbol{\gamma} - \boldsymbol{\gamma}_h\|_0 \leq C\big(\|\boldsymbol{\phi} - \boldsymbol{\phi}_I\|_1 + t\|\boldsymbol{\gamma} - \boldsymbol{\gamma}_I\|_0 + h\|\boldsymbol{\gamma}\|_0\big).$$

Suppose in addition that for $s \geq 2$, $(\boldsymbol{\gamma} - \boldsymbol{R}_h \boldsymbol{\gamma}, \eta) = 0 \quad \forall \eta \in \boldsymbol{P}_{s-2}$, where $\boldsymbol{P}_k$ denotes discontinuous piecewise polynomials vectors of degree $\leq k$. Then, letting $\boldsymbol{\Pi}$ denote $\boldsymbol{L}^2$ projection into $\boldsymbol{P}_{s-2}$,

$$\|\boldsymbol{\phi} - \boldsymbol{\phi}_h\|_1 + t\|\boldsymbol{\gamma} - \boldsymbol{\gamma}_h\|_0 \leq C\big(\|\boldsymbol{\phi} - \boldsymbol{\phi}_I\|_1 + t\|\boldsymbol{\gamma} - \boldsymbol{\gamma}_I\|_0 + h\|\boldsymbol{\gamma} - \boldsymbol{\Pi}\boldsymbol{\gamma}\|_0\big).$$

To apply this result, find approximations ω_I and $\boldsymbol{\phi}_I$ which satisfy:

$$\mathbf{grad}\,\omega_I - \boldsymbol{R}_h \boldsymbol{\phi}_I = \boldsymbol{R}_h\,\mathbf{grad}\,\omega - \boldsymbol{R}_h \boldsymbol{\phi}$$

and

$$\|\boldsymbol{\phi} - \boldsymbol{\phi}_I\|_0 + h\|\boldsymbol{\phi} - \boldsymbol{\phi}_I\|_1 \leq Ch^{s+1}\|\boldsymbol{\phi}\|_{s+1}, \qquad \|\boldsymbol{\gamma} - \boldsymbol{R}_h \boldsymbol{\gamma}\|_0 \leq Ch^s\|\boldsymbol{\gamma}\|_s.$$

If so, then

$$\boldsymbol{\gamma}_I = t^{-2}(\mathbf{grad}\,\omega_I - \boldsymbol{R}_h \boldsymbol{\phi}_I) = t^{-2}\boldsymbol{R}_h(\mathbf{grad}\,\omega - \boldsymbol{\phi}) = \boldsymbol{R}_h \boldsymbol{\gamma}.$$

Hence, we obtain for $s \geq 1$

$$\|\boldsymbol{\phi} - \boldsymbol{\phi}_h\|_1 + t\|\boldsymbol{\gamma} - \boldsymbol{\gamma}_h\|_0 \leq Ch^s\big(\|\boldsymbol{\phi}\|_{s+1} + \|\boldsymbol{\gamma}\|_{s-1} + t\|\boldsymbol{\gamma}\|_s\big),$$

where the constant C is independent of h and t. Note, however, that the norms on the right hand side of the estimate are NOT independent of t for $s \geq 3/2$.

Leaving aside the question of how we construct such special interpolants, we concentrate on what such an estimate tells us about the best possible order of convergence that is achievable. Although this theorem only provides an upper bound on the error, it indicates that the error in the approximation of the rotation $\boldsymbol{\phi}$ and the shear stress $\boldsymbol{\gamma}$ depend on the simultaneous approximation of both these variables. A typical error estimate for the approximation of ω indicates that this error depends on the approimation properties of $\boldsymbol{\Theta}_h$ and $\boldsymbol{\Gamma}_h$, as well as W_h. So a natural question to ask is what is known about such approximations on quadrilaterals.

4 Approximation Theory

We look first at the case of scalar approximation on rectangular meshes, Given a subspace $\hat{S}$ of $L^2(\hat{K})$, we define the associated subspace on an arbitrary square K by

$$S(K) = \{\, u : K \to \mathbb{R} \,|\, \hat{u}_K \in \hat{S} \,\}.$$

For $n = 1, 2, \ldots$, let τ_h be the uniform mesh of the unit square Ω into n^2 subsquares when $h = 1/n$, and define

$$S_h = \{\, u : \Omega \to \mathbb{R} \,|\, u|_K \in S(K) \text{ for all } K \in \tau_h \,\}.$$

Then the following well-known result gives a set of equivalent conditions for optimal order convergence (e.g., see [1]).

Theorem 4.1 *Let $\hat{S}$ be a finite dimensional subspace of $L^2(\hat{K})$, r a non-negative integer. The following conditions are equivalent:*

$$\textit{There is a constant } C \textit{ such that } \inf_{v \in S_h} \|u - v\|_{L^2(\Omega)} \leq Ch^{r+1}|u|_{H^{r+1}(\Omega)} \quad \textit{for all } u \in H^{r+1}(\Omega). \tag{4.1}$$

$$\inf_{v \in S_h} \|u - v\|_{L^2(\Omega)} = o(h^r) \quad \textit{for all } u \in P_r(\Omega). \tag{4.2}$$

$$P_r(\hat{K}) \subset \hat{S}. \tag{4.3}$$

Hence, for optimal order approximation, one needs to have $P_r(\hat{K}) \subset \hat{S}$. For optimal order approximation on quadrilaterals, however, a stronger condition is needed. To state the result, we recall that a family τ_h of decompositions of Ω into quadrilaterals K is called shape-regular (cf. [9]) if all the quadrilaterals are convex and there exist constants $\sigma \geq 1$ and $0 < \rho < 1$ independent of h such that

$$h_K/h_K^{'} \leq \sigma, \quad |\cos\theta_{iK}| \leq \rho, \quad i = 1, 2, 3, 4, \quad \forall K \in \tau_h,$$

where h_K, $h_K^{'}$, and θ_{iK} are the diameter of K, the smallest length of the sides of K, and the angles of K, respectively.

The following result is established in [1].

Theorem 4.2 *Let τ_h denote a shape-regular sequence of quadrilateral meshes of a two-dimensional domain Ω, where h denotes the maximum diameter of the elements $K \in \tau_h$. Let V^{τ_h} denote the space of functions on Ω which belong to $V_{F_K}(K)$ when restricted to a generic quadrilateral $K \in \tau_h$. Then a necessary condition for the estimate* (4.2) *to hold is that $Q_r \subseteq \hat{V}$.*

Recall that the natural way to preserve the condition $\mathbf{grad}\, W_h \subseteq \mathbf{\Gamma}_h$ is to define $\mathbf{\Gamma}_h$ by mapping spaces defined on the reference square to the general quadrilateral using the rotated version of the Piola transform. To state the analogue of Theorem 4.2 for such spaces, we introduce the following notation. Denote by $\boldsymbol{RT}_r$ the span of the space $\hat{\boldsymbol{V}}$ associated to the rotated Raviart–Thomas space of order r defined on the reference element. We recall that $\boldsymbol{RT}_r = P_{r,r+1} \times P_{r+1,r}$. In particular, the Raviart–Thomas shape functions on the reference element are the span of the vectors $(\hat{x}^i\hat{y}^j, 0)$, $0 \leq i \leq r$, $0 \leq j \leq r+1$ and $(0, \hat{x}^i\hat{y}^j)$, $0 \leq i \leq r+1$, $0 \leq j \leq r$. We then define the space $\boldsymbol{S}_r$ to be the span of the vectors given above, but where the vectors $(\hat{x}^r\hat{y}^{r+1}, 0)$ and $(0, \hat{x}^{r+1}\hat{y}^r)$ are replaced by the single vector $(\hat{x}^r\hat{y}^{r+1}, \hat{x}^{r+1}\hat{y}^r)$. Thus, $\boldsymbol{RT}_r$ is equal to the span of $\boldsymbol{S}_r$ and the vector $(\hat{x}^r\hat{y}^{r+1}, -\hat{x}^{r+1}\hat{y}^r)$. For $r = 1, 2, \ldots$, we also define R_r to be the span of the monomials $\hat{x}^i\hat{y}^j$, $i, j = 0, \ldots r$, but omitting the monomial $\hat{x}^r\hat{y}^r$.

Theorem 4.3 *Let τ_h denote a shape-regular sequence of quadrilateral meshes of a two-dimensional domain Ω, where h denotes the maximum diameter of the elements $K \in \tau_h$. Let $\boldsymbol{V}^{\tau_h}$ denote the space of vectorfields on Ω which belong to $\boldsymbol{V}_{F_K}(K)$ when restricted to a generic quadrilateral $K \in \tau_h$. Then a necessary condition for the estimate*

$$\inf_{\boldsymbol{\eta} \in \boldsymbol{V}^{\tau_h}} \|\boldsymbol{\gamma} - \boldsymbol{\eta}\|_{L^2(\Omega)} = o(h^r) \quad \textit{for all } \boldsymbol{\gamma} \in P_r(\Omega, \mathbb{R}^2)$$

to hold is that $\boldsymbol{S}_r \subseteq \hat{\boldsymbol{V}}$ and a necessary condition for the estimate

$$\inf_{\boldsymbol{\eta} \in \boldsymbol{V}^{\tau_h}} \|\mathrm{rot}[\boldsymbol{\gamma} - \boldsymbol{\eta}]\|_{L^2(\Omega)} = o(h^r) \quad \textit{for all } \boldsymbol{\gamma} \textit{ with } \mathrm{rot}\, \boldsymbol{\gamma} \in P_r(\Omega)$$

to hold is that $R_{r+1} \subseteq \hat{\mathrm{rot}}\, \hat{\boldsymbol{V}}$.

A proof of the analogue of this result for finite element subpaces of $H(\mathrm{div})$ can be found in [2].

A key ingredient in establishing Theorem 4.2 is to first show that for $P_r(K)$ to belong to $V_F(K)$, we must have $Q_r(\hat{K}) \in \hat{V}$. Analogously, a key ingredient in establishing Theorem 4.3 is to first show that for $P_r(K, \mathbb{R}^2)$ to belong to $\boldsymbol{V}_F(K)$, we must have $\boldsymbol{S}_r \in \hat{\boldsymbol{V}}$.

5 Implications for quadrilateral Reissner-Mindlin elements

The MITC4 and Durán-Liberman elements both use the full Q_1 space to approximate both $\boldsymbol{\theta}$ and ω and the full $\boldsymbol{RT}_0$ space to approximate $\boldsymbol{\gamma}$. Since $\boldsymbol{RT}_0 \subseteq \boldsymbol{S}_0$, we do not expect degradation of convergence rate in going from a rectangular mesh to a shape-regular quadrilateral mesh. Both of these methods have been analyed in a recent paper [10]. The quadrilateral version of the Durán-Liberman scheme is shown to converge with optimal order $O(h)$ on shape-regular meshes, while for the MITC4 method, this result is only obtained for asymptotically parallelogram meshes. However, numerical experiments do not indicate any degradation of convergence rates, even for more general shape-regular quadrilateral meshes.

The nonconforming element of Ye approximates ω by a space for which $\hat{V}$ does not contain all of Q_1 (cf. [13] for further discussion of this space). Thus, we would expect to see a degradation of convergence rate in the approximation of ω. One possible remedy for this is to add the nonconforming bubble $(\hat{x} - 1/2)(\hat{y} - 1/2)$ to the set of basis functions on the reference element for the space W_h and the gradient of this function to the reference element for the space $\boldsymbol{\Gamma}_h$. However, when this is done, certain key properties which hold for the case of rectangles no longer hold for quadrilaterals, so the extension of the analysis to the quadrilateral case is not clear.

The MITC8 element approximates both $\boldsymbol{\theta}$ and ω by spaces obtained from mappings of the quadratic serentipity space. Since this space does not contain all of Q_2, (i.e, it is missing the basis function x^2y^2), we expect to see only $O(h)$ convergence. The space $\boldsymbol{\Gamma}_h$ is obtained by mapping the $\boldsymbol{BDM}_1$ space. Since this space does not contain $\boldsymbol{S}_1$, we also expect this to be a cause of degradation of convergence.

The MITC9 element uses the full Q_2 approximation for $\boldsymbol{\theta}$, but the use of the Q_2 serendipity space to approximate ω and the $\boldsymbol{BDFM}_2$ space (which does not contain $\boldsymbol{S}_1$) to approximate $\boldsymbol{\gamma}$ will cause degradation in the convergence rate.

On the other hand, we expect the space MITC12 to suffer no degradation of convergence on shape-regular quadrilateral meshes as a result of suboptimal approximation by the subspaces. Of course, the analysis of such methods is quite delicate, so optimal order approximation by the finite element subspaces is not the only issue in establishing optimal order convergence rates.

Finally, we remark that the degradation of convergence rates noted above for approximation on general quadrilateral meshes by certain families of finite elements does not occur for meshes of parallelograms or even for meshes whose elements are sufficiently close to parallelograms. In particular, if we begin with any mesh of convex quadrilaterals, and continually refine it by dividing each quadrilateral in four by connecting the midpoints of the opposite edges, the resulting sequence of meshes is asymptotically parallelogram and shape-regular. It was shown in [1] that for such meshes in the case of scalar finite element approximation, if the reference space contains only $P_r(\hat{K})$, rather than $Q_r(\hat{K})$, one still has optimal $O(h^{r+1})$ convergence in L^2. Since such meshes occur commonly in practice, this may explain why the degradation of convergence rate is not observed more often.

References

[1] D.N. Arnold, D. Boffi, R.S. Falk, *Approximation by quadrilateral finite elements*, Math. Comp., to appear.

[2] D.N. Arnold, D. Boffi, R.S. Falk, *Quadrilateral H(div) finite elements*, preprint.

[3] D.N. Arnold, R.S. Falk, *Uniformly accurate finite element method for the Reissner–Mindlin plate*, SIAM J. Numer. Anal. **26** (1989), no. 6, 1276–1290.

[4] K.J. Bathe, F. Brezzi, M. Fortin, *Mixed-interpolated elements for Reissner–Mindlin plates*, Internat. J. Numer. Methods Engrg. **28** (1989), 1787–1801.

[5] K.J. Bathe, E. Dvorkin, *A four node plate bending element based on Mindlin–Reissner plate theory and mixed interpolation*, Internat. J. Numer. Methods Engrg. **21** (1985), 367–383.

[6] K.J. Bathe, E. Dvorkin, *A formulation of general shell elements–The use of mixed interpolation of tensorial components*, Internat. J. Numer. Methods Engrg. **22** (1986), 697–722.

[7] F. Brezzi, M. Fortin, *Mixed and hybrid finite element methods*, Springer-Verlag, New York, 1991.

[8] F. Brezzi, M. Fortin, R. Stenberg, *Error analysis of mixed-interpolated elements for Reissner–Mindlin plates*, Math. Models Methods Appl. Sci., 1 (1991), 125–151.

[9] P.G. Ciarlet, *The Finite Element Method for Elliptic Problems*, North-Holland, Amsterdam, 1978.

[10] R. Durán, E. Hernández, L. Hervella-Nieto, E. Liberman, R. Rodriguez, *Error estimates for low-order isoparametric quadrilateral finite elements for plates*, preprint, (2002), 1–22.

[11] R. Durán, E. Liberman, *On mixed finite element methods for the Reissner–Mindlin plate model*, Math. Comp., 58 (1992), no. 198, 561–573.

[12] R.S. Falk, T. Tu, *Locking-free finite elements for the Reissner-Mindlin plate*, Math. Comp., 69 (2000), 911-928.

[13] R. Rannacher, S. Turek, *Simple nonconforming quadrilateral Stokes elements*, Numer. Meth. Part. Diff. Equations, 8 (1992), 97–111.

[14] R. Stenberg, M. Suri, *An hp-analysis of MITC plate elements*, SIAM J. Numer. Anal., 34 (1997), no. 2, 544–568.

[15] X. Ye, *A rectangular element for the Reissner–Mindlin plate*, Numer. Methods Partial Differential Equations, 16 (2000), no 2, 184–193.